

Nondestructive evaluation of elastic parameters of sintered iron powder compacts

J. P. PANAKKAL*, H. WILLEMS, W. ARNOLD,
Fraunhofer Institute for NDT D-6600 Saarbrücken 11, FRG

A systematic study of the variation of elastic moduli and Poisson's ratio of sintered iron compacts of porosity (up to 21.6%) has been carried out by measuring longitudinal and shear ultrasonic velocities. The variation of these parameters with porosity is compared with predictions of elasticity and scattering theories. Further, a linear relationship was observed between the elastic moduli and the ultrasonic velocities and the use of ultrasonic velocity as a predictor of elastic moduli is therefore recommended for porous materials.

1. Introduction

Characterization of sintered powder metal parts and ceramics using ultrasonics has been widely reported in the literature [1-3]. Nondestructive evaluation of elastic moduli of these parameters at different stages of fabrication would help in improving the quality of the final product. Elastic moduli and Poisson's ratio of sintered iron compacts (different compaction pressures and sintering cycles) have been evaluated as a function of porosity (up to 21.6%) using ultrasonics. Analysis of the data indicates that ultrasonic velocity itself can be used for monitoring the elastic moduli of porous materials without measuring density. This paper presents the experimental details and analysis of the data generated and compares the results with theory.

2. Experimental details

2.1. Specimens

Iron compacts (sintered and hot isostatic pressed) were supplied by Institute for Physical Chemistry, Vienna University. The details of the fabrication parameters are presented in Table I. Cut specimens of diameter ~ 9 mm and thickness ~ 3 mm having a plane parallelism better than $2 \mu\text{m}$ were used for the nondestructive evaluation of elastic moduli.

2.2. Ultrasonic measurement

Ultrasonic velocity (longitudinal and shear) of these specimens was measured using cross-correlation method [4, 5]. The experimental set up used is shown in Fig. 1. The centre frequency of the transducers (6.25 mm dia.) used was 5 MHz and the measurement was carried out with a buffer rod. The backwall echoes were digitized and cross correlation function of two selected echoes was obtained by means of an implemented software package. The displacement of the cross-correlation function in the time domain gave the transit time. Details of the cross-correlation technique used is being reported elsewhere [5]. The transit time was determined with an accuracy of

± 1 nsec. The longitudinal velocity of each of the 20 specimens was measured six times and the average was taken for evaluation. Shear velocity was measured with the plane of polarization in two perpendicular directions and the average of three sets of measurement was considered for calculation. The variation of shear velocity polarized in two perpendicular directions for the specimens was generally less than 0.5%.

3. Results

The elastic moduli are given by the following equations:

$$\text{Young's modulus } E = \rho V_s^2 (3V_l^2 - 4V_s^2) / (V_l^2 - V_s^2) \quad (1a)$$

$$\text{Shear modulus } G = \rho V_s^2 \quad (1b)$$

$$\text{Poisson's ratio } \nu = (V_l^2/2 - V_s^2)/(V_l^2 - V_s^2) \quad (1c)$$

where ρ is density,
 V_l is longitudinal velocity, and
 V_s is shear velocity.

3.1. Variation of elastic parameters with porosity

Figure 2 presents a plot of Young's and shear moduli as a function of pore volume fraction p .

In the literature, different forms of equations have been proposed for the behaviour of elastic moduli with porosity in porous materials [6-10]. A least square analysis of the data was carried out to fit into the following commonly used equations:

$$E = E_0 \exp(-ap), \quad (2a)$$

$$\frac{1}{E} = \frac{1}{E_0} + B \frac{p}{(1-p)}, \quad (2b)$$

$$E = E_0 \exp[-(bp + cp^2)] \quad (2c)$$

where a , b , c and B are constants.

* Present address: Prefre Expansion Project, Bhabha Atomic Research Centre, Tarapur-Ghivali (PO), Thane District, Maharashtra State 401502, India.

TABLE I Fabrication parameters of the investigated iron compacts

No. and symbol	Compaction pressure (MPa)	Sintering		Pore volume (%)
		Temperature (K)	Time (h)	
1 ○	400	1523	0.5	12.7
2 △	600	1523	0.5	7.7
3 □	1200	1523	0.5	4.1
4 ○	400	1523	2	12.2
5 △	600	1523	2	7.7
6 □	1200	1523	2	4.0
7 ○	400	1523	8	12.0
8 △	600	1523	8	7.4
9 □	1200	1523	8	3.5
10 ●	400	1393	0.5	12.6
11 ▲	600	1393	0.5	7.8
12 ■	1200	1393	0.5	3.2
13 ●	400	1393	2.0	12.4
14 ▲	600	1393	2.0	7.8
15 ■	1200	1393	2.0	3.0
16 ●	400	1393	8.0	12.1
17 ▲	600	1393	8.0	7.8
18 ■	1200	1393	8.0	3
19 ▽	HIP			
20 ▼	200	1250	1.0	21.6

Table II presents the extrapolated values of the elastic moduli for nonporous material from the above equations and values of electrolytic iron [11]. It can be seen from Fig. 2 that the Equation 2c gives the best fit with a coefficient of correlation better than 0.99 similar to the studies of alumina [12]. The equation of this form has been derived using a phenomenological model and elasticity theory [8].

Figure 3 presents the values of Poisson's ratio of the specimens as a function of pore volume fraction p . Attempts to fit all the 20 data points to linear, exponential and second degree equation in porosity results in either error for the value of nonporous material or lower value of correlation coefficient. The data was therefore fitted omitting the value for the largest pore fraction (0.216) yielding a correlation coefficient better than 0.99 for the equations below.

$$v = 0.291 (1 - 0.80p)$$

$$v = 0.292 (\exp - 0.85p)$$

3.2. Theoretical predictions

3.2.1. Elasticity theory

The elastic moduli in porous materials containing spherical pores have been derived by a number of authors from the elasticity considerations [9, 13]. At

lower range of pore volume fraction ($p \leq 0.05$), a linear relationship between the moduli and the porosity has been predicted. The following simple relations can be derived from the treatment given in reference [13].

$$E = E_o (1 - C_E p), \tag{4a}$$

$$G = G_o (1 - C_G p), \tag{4b}$$

$$V_l = V_{l_o} (1 - C_l p), \tag{4c}$$

$$V_s = V_{s_o} (1 - C_s p), \tag{4d}$$

$$v = v_o (1 - C_v p), \tag{4e}$$

where

$$C_E = 1/18 (29 + 11v_o),$$

$$C_G = 5/3,$$

$$C_v = 5/9 + 11v_o/18 - 1/(18v_o),$$

$$C_l = 1/2 \{ C_E + 2C_v v_o^2 (2 - v_o) / [(1 - v_o)(1 + v_o) \cdot (1 - 2v_o)] - 1 \},$$

$$C_s = 1/3.$$

The subscript 'o' denotes nonporous material.

The dashed line in Figs 3 and 4 give the calculated values from the above equations. The deviation from

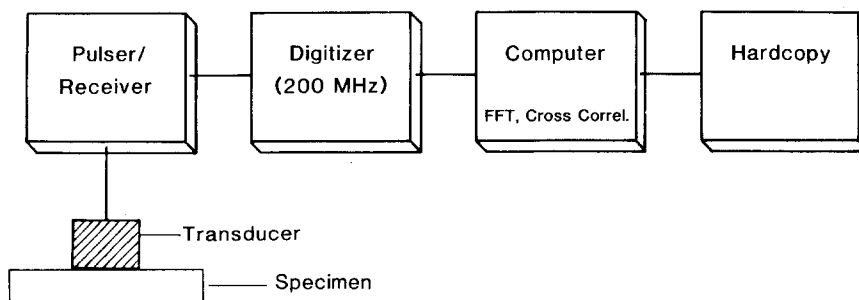


Figure 1 Measurement of ultrasonic velocity by cross-correlation technique schematic.

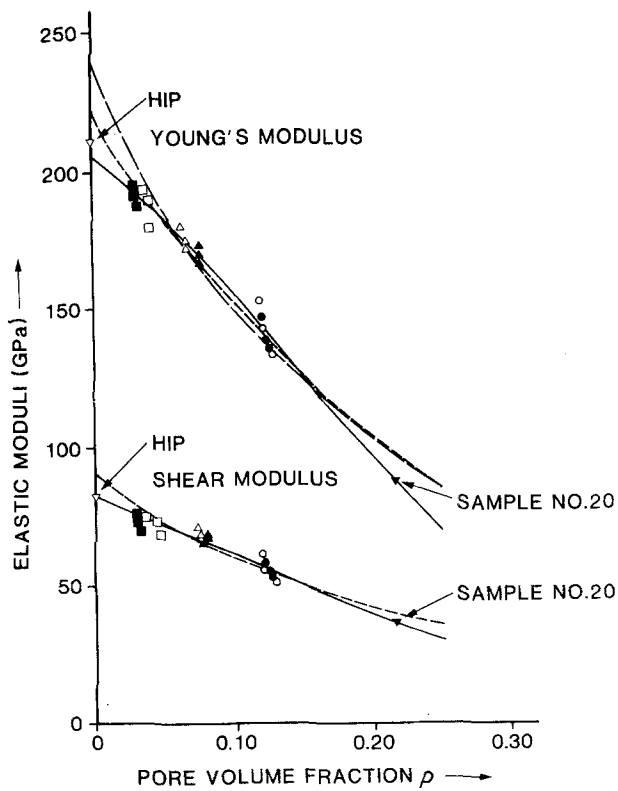


Figure 2 Variation of elastic moduli with pore volume fraction p (---) $E = E_0 \exp(-ap)$ [6], (---) $1/E = 1/E_0 + Bp/(1-p)$ Hashin's equation [7], (—) $E = E_0 \exp[-(bp + cp^2)]$ [8]. Compaction pressures: (○) 400 MPa; (△) 600 MPa; (□) 1200 MPa. Full symbols, sintered at 1393 K and empty symbols, 1523 K.

the theoretical values increases as pore volume increases. This is expected because the pores become less spherical and become interconnected at higher porosity. This is evident from the photomicrographs of some typical samples (Fig. 5). Further the deviation is minimum if the moduli (the largest value) at any compaction pressure corresponding to maximum sintering time (8 h) are considered in Fig. 4. The values calculated from other models based on elasticity theory generally agree with these values [7, 9].

A different approach (powder metallurgy model) has been reported for ceramics assuming a simple cubic stacking of spherical powder particles [12]. During densification, the flat contact areas of the spheres increase until the residual spherical surfaces shrink into points. Expressions have been derived considering the behaviour of the unit cell of the cubic array subjected to stress. This powder metallurgy

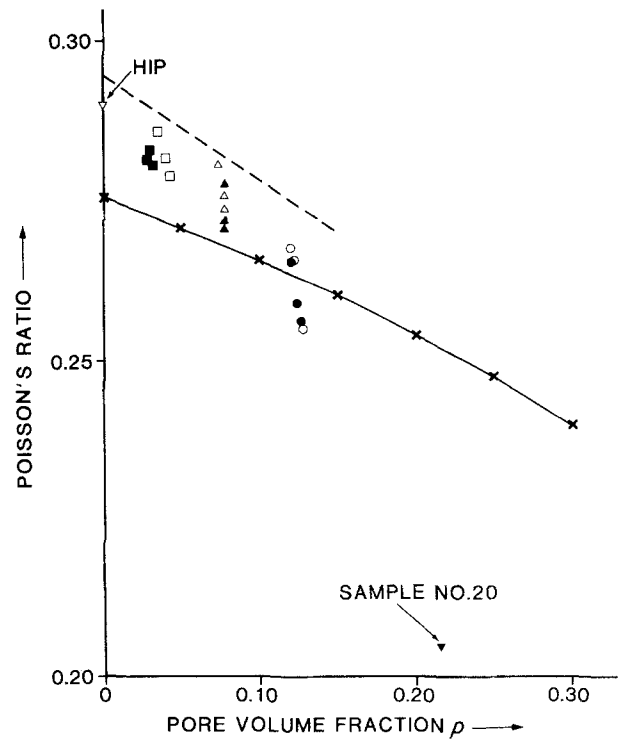


Figure 3 Variation of Poisson's ratio with pore volume (---) elasticity theory, (-x-x-x) scattering theory.

approach gives the following equations

$$\begin{aligned} E &= E_0 \exp[-(bp + cp^2)] \\ G &= G_0 \exp[-(bp + cp^2)] \end{aligned} \quad (5)$$

where $b = 3.35$ and $c = 5.48$ as approximate equations to the exact solution for both Young's modulus and shear modulus.

The values of elastic moduli calculated, for the powder metallurgy model gives generally lower values (Fig. 4). Compared to the other models, the agreement is good over the whole range. The deviation observed arises because of two reasons:

1. the irregular stacking pattern of the initial powders present in practice as against the assumed simple cubic pattern;
2. the presence of nonspherical powders instead of spherical powders.

3.2.2. Self-consistent scattering theory

The self-consistent treatment of multiple scattering assumes the two types of scatterers to be deviations

TABLE II Least square fitting of experimental values of elastic moduli

Equation	Modulus (GPa)	Constants				Coefficient of correlation, r
		a	b	c	B	
$E = E_0 \exp(-ap)$	$E = 223$	3.77				0.97
$G = G_0 \exp(-ap)$	$G_0 = 86$	3.50				0.97
$\frac{1}{E} = \frac{1}{E_0} + Bp/(1-p)$	$E_0 = 236$				0.218	0.96
$\frac{1}{G} = \frac{1}{G_0} + Bp/(1-p)$	$G_0 = 91$				0.513	0.96
$E = E_0 \exp[-(bp + cp^2)]$	$E_0 = 207$		1.68	10.5		0.99
	$G_0 = 80$		1.73	8.9		0.99
Electrolytic iron	$E_0 = 212$ $G_0 = 82$					

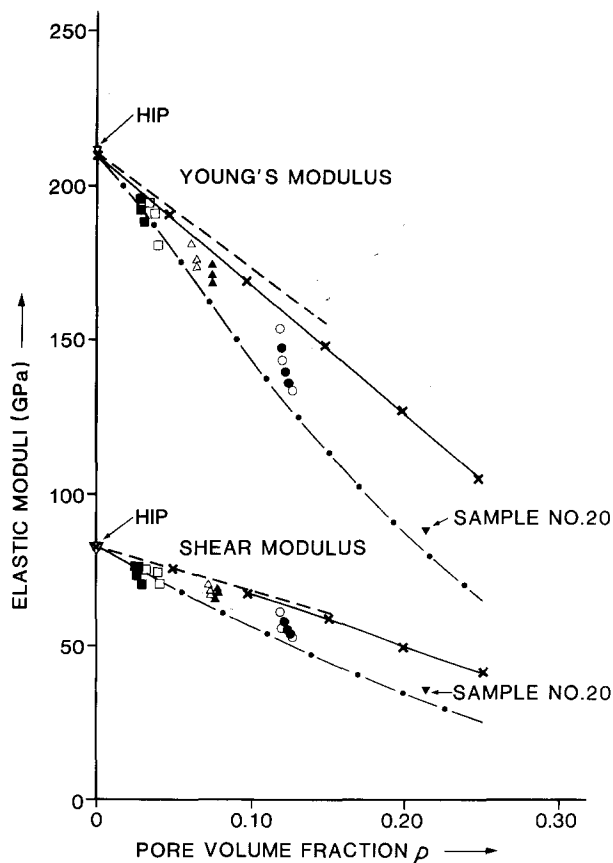


Figure 4 Elastic moduli against pore volume fraction, comparison with theory (---) elasticity theory, (-x-x-x) scattering theory, (.....) powder metallurgy model.

from the effective properties of the medium. The elastic moduli as a function of porosity were calculated solving the equations reported [14]. The agreement with the measured values is better than the conventional elasticity theory (Equation 4). The deviation at higher porosity arises from the nonspherical nature of the pores, especially in sintered metal parts [14].

3.2.3. Poisson's ratio

Poisson's ratio as a function of porosity are also calculated from the above two formalisms and is presented in Fig. 3 for comparison. The values from powder metallurgy model were not calculated since it assumes a constant value of Poisson's ratio. Neither theory shows good agreement with measured values. This is not very surprising considering the fact Poisson's ratio is a small quantity dependent on the differences of the other elastic properties and is very sensitive to errors in them as observed earlier based on a comparison of experimental data of a number of ceramics and theory [9].

4. Discussion

On a comparison of the experimental values of elastic moduli and the calculated values, the powder metallurgy model and the self-consistent scattering theories come closest to the measured values. The agreement of the powder metallurgy model is better at higher porosity as it is inherently capable of treating the transition of the pore structure from interconnected to isolated pores. The scattering theory treats pores as isolated spherical scatterers. The elasticity equations used, however are valid only at a lower range of porosity.

It is well known that the elastic moduli of porous material depend on porosity. But the moduli change as a function of pore shape and pore structure [9] which in turn depend on the characteristics of initial powders and fabrication parameters like compaction pressure, sintering temperature and time. Ultrasonic velocity is also a function of porosity in a broader sense. But at any level of porosity, the velocity is not a unique function of porosity and it depends on the

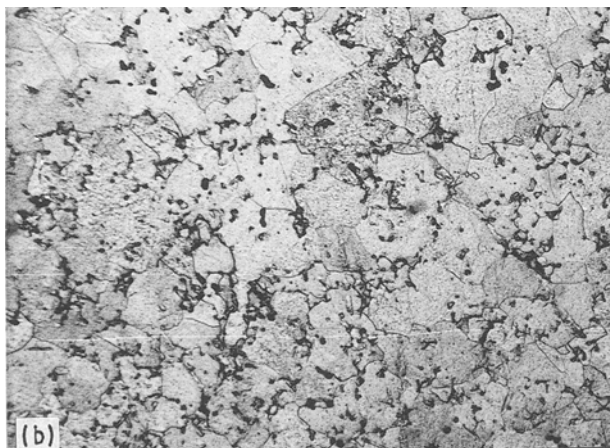
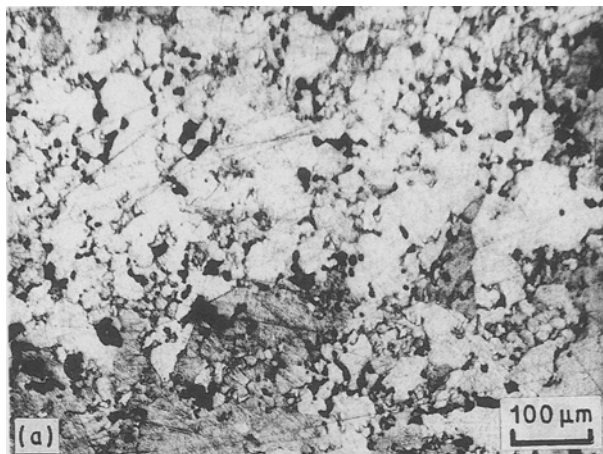


Figure 5 Photomicrographs of sintered iron compacts with different pore volume fraction p (a) sample no. 20, $p = 0.216$; (b) sample no. 16, $p = 0.121$; (c) sample no. 18, $p = 0.03$.



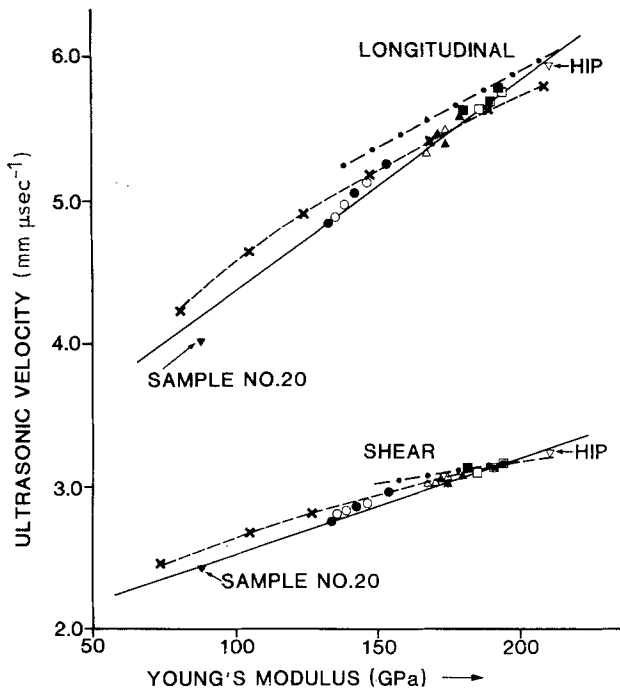


Figure 6 Plot of ultrasonic velocity against Young's modulus (—) least square fit, (-·-·-·) elasticity theory, (x-x-x) scattering theory.

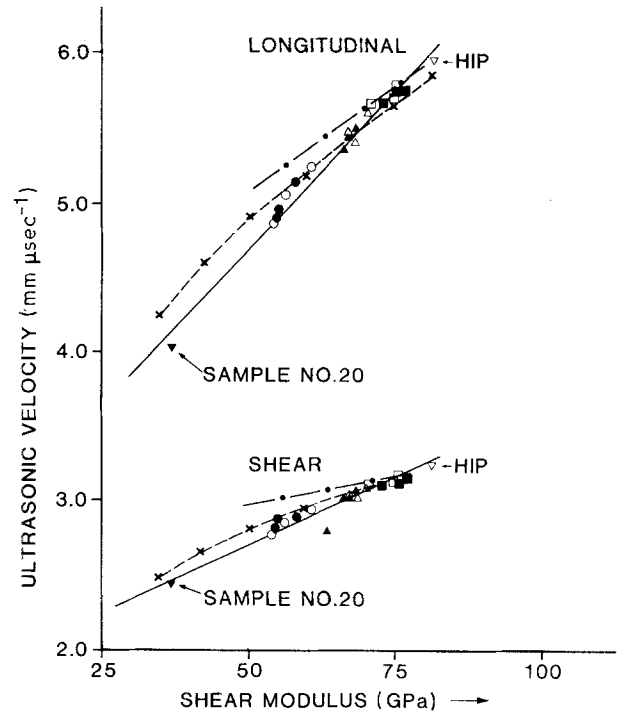


Figure 7 Plot of ultrasonic velocity against shear modulus (—) least square fit, (-·-·-·) elasticity theory, (x-x-x) scattering theory.

pore shape and orientation [15]. An attempt was therefore made to see whether there exists any relationship between the moduli of the compacts and the ultrasonic velocity due to changes in the shape, size and distribution of pores arising from different fabrication parameters.

Figures 6 and 7 present the plot of the elastic moduli (E and G) and the ultrasonic velocities. The solid line indicates least square fit of the data given by the following equations with a coefficient of correlation of 0.99.

$$E = 204 - 65 (V_{10} - V_1) \quad (6a)$$

$$E = 203 - 158 (V_{s0} - V_s) \quad (6b)$$

$$G = 79 - 24 (V_{10} - V_1) \quad (6c)$$

$$G = 77 - 58 (V_{s0} - V_s) \quad (6d)$$

The good correlation between the moduli and the velocities suggests that the effect of the pore shape, size and structure due to the variation of fabrication parameters on the elastic moduli is manifested in the same way in the ultrasonic velocity also.

The set of equations (Equation 6) can be rewritten in the form

$$M = M_0 - C(V_0 - V) \quad (7)$$

where M is the modulus, C is a constant and V is the ultrasonic velocity. According to elasticity theory, the modulus and the velocity are linear functions of pore volume fraction p (Fig. 4a to d). By simple rearrangement and substituting p , the following relation is derived

$$M = M_0 - M_0 C_M / (V_0 C_V) (V_0 - V) \quad (8)$$

The calculated moduli are indicated by a dashed-dotted line in Figs 6 and 7.

The slopes depend on the constants C_E , C_{V1} , C_{Vs} , C_G and C_s which are calculated from elasticity theory (Equation 4). Since these constants themselves differed in numerical values, the slopes of the calculated values of velocity for a particular modulus would be different. However, the slopes are nearly the same if the values are calculated assuming experimental values of these constants. The purpose of the discussion about the elasticity theory is to show that a linear relationship between the modulus and velocity is expected for lower pore volumes.

On the other hand, scattering theory gives a better agreement with the observed results. Further the variation is linear upto a pore volume fraction ≈ 0.15 corresponding to a change of elastic moduli by 50%.

A similar relationship is also observed in α -silicon carbide samples in the density range of 3.005 to 3.209 g cm^{-3} (93.6 to 99.9% of theoretical density). Young's modulus of hot isostatic pressed samples (60) in the density range 3.142 to 3.209 g cm^{-3} had been recently evaluated from the ultrasonic velocity values (longitudinal and shear) at Fraunhofer-Institute for NDT, Saarbrücken [16]. The reported data of six sintered samples in the density range of 3.005 to 3.134 g cm^{-3} is also used for the analysis [17].

Figure 8 presents the plot of longitudinal ultrasonic velocity against Young's modulus. The data points (66 pairs) were fitted into a straight line of the form given by Equation 7 by the method of least squares (coefficient of correlation $r = 0.97$), giving

$$E = 458 - 93 (12.352 - V_l) \quad (9)$$

Both these examples suggest that the linear relationship between Young's modulus and longitudinal ultrasonic velocity may be used as a simple non-

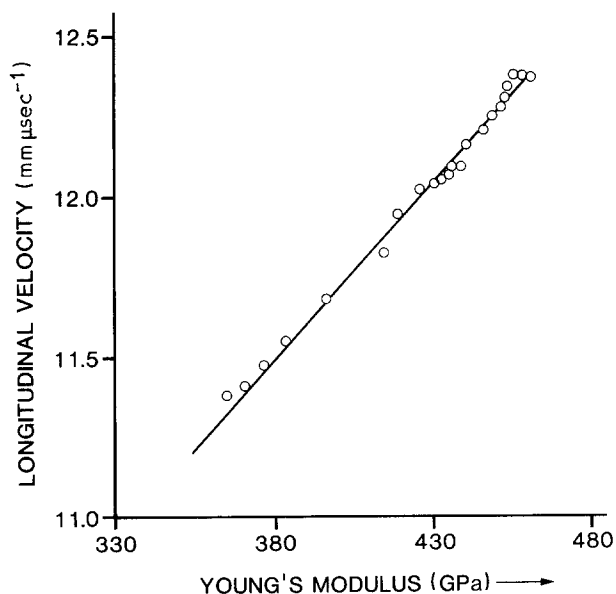


Figure 8 Plot of longitudinal ultrasonic velocity against Young's modulus of α -silicon carbide.

destructive technique for evaluating the elastic moduli of porous material without measuring density. The agreement using the results obtained from hot isostatic pressed samples and sintered samples of α -silicon carbide in two different laboratories give more confidence to the application of this technique as a routine check for monitoring elastic moduli for porous materials in a fabrication plant.

5. Conclusion

Elastic moduli and Poisson's ratio of sintered iron compacts were evaluated as a function of porosity from the ultrasonic velocities. The observed variation of the elastic parameters was compared with theoretical predictions of both elasticity and scattering theories. Large deviation was observed at high porosities and short sintering cycles, due to non-spherical shape of the pores. Scattering theory and powder metallurgy model generally show better agreement with the results of the experimental investigation. The powder metallurgy model, however shows better agreement at high porosity. A more rigorous model which takes into account the change of pore shape size and structure as the level of porosity

changes during sintering would be able to explain the experimental data better. Data analysis of the results indicate that ultrasonic velocity preferably longitudinal velocity, may be used to evaluate the elastic moduli of porous materials. Basis for this observation has been shown from elasticity and scattering theories.

Acknowledgements

The authors would like to thank Dr W Hessler, Institute for Physical Chemistry of Vienna University, for providing the specimens. The financial support received by the first author from Kernforschungsanlage (KFA) Jülich during this work is gratefully acknowledged.

References

1. E. P. PAPADAKIS and B. W. PATERSEN, *Mat. Eval.* **37** (1979) 76.
2. R. M. ARONS and D. S. KUPPERMAN, *ibid.* **40** (1982) 1076.
3. J. P. PANAKKAL, J. K. GHOSH and P. R. ROY, *J. Phy. D.: Applied Physics* **17** (1984) 1791.
4. D. R. HULL, H. E. KAUTZ and A. VARY, *Mat. Eval.* **43** (1985) 1455.
5. J. P. PANAKKAL, H. PEUKERT and H. WILLEMS, in Proceedings 3rd International Symposium on Nondestructive Characterization of Materials, 3-6 October, 1988, Saarbrücken, Federal Republic of Germany (in press).
6. R. SPRIGGS, *J. Amer. Ceram. Soc.* **44** (1961) 628.
7. Z. HASHIN, *J. Appl. Mech.* **29** (1962) 143.
8. JAMES C. WANG, *J. Mater. Sci.* **19** (1984) 801.
9. R. W. RICE, in Treatise on Material Science and Technology, edited by R. K. MacCrone (Academic Press, New York, 1977) Vol. 11, p. 199.
10. J. E. BAILEY and N. A. HILL, *Proc. Brit. Ceram. Soc.* **15** (1979) 15.
11. Standard No. E494 in Annual Book of ASTM Standards, Vol. 03.03. Metallography, Nondestructive Testing (ASTM, Philadelphia, 1983) p. 483.
12. JAMES C. WANG, *J. Mater. Sci.* **19** (1984) 809.
13. G. ONDRACEK, *Z. Werkstofftech.* **9** (1978) 31.
14. C. M. SAYERS and R. L. SMITH, *Ultrasonics* **19** (1982) 201.
15. W. KREHER, J. RANACHOWSKI and F. REJMUND, *ibid.* **14** (1977) 70.
16. H. REITER, B. HOFFMANN, A. MORSCH, W. ARNOLD and E. SCHNEIDER, IzfP Report No. 880335-TW (1988).
17. J. J. GRUBER, J. M. SMITH and R. H. BROCKELMAN, *Mat. Eval.* **46** (1988) 98.

Received 3 January
and accepted 14 April 1989